IEEE Access
Multidisciplinary | Rapid Review | Open Access Journal

Received 5 September 2023, accepted 29 September 2023, date of publication 4 October 2023, date of current version 11 October 2023.

Digital Object Identifier 10.1109/ACCESS.2023.3321829

RESEARCH ARTICLE

A Proposal of an Axial-Flux Permanent-Magnet Machine Employing SMC Core With Tooth-Tips Constructed by One-Pressing Process: Improving Torque and Manufacturability

REN TSUNATA[1], (Member, IEEE), MASATSUGU TAKEMOTO[1], (Member, IEEE), JUN IMAI[1], (Member, IEEE), TATSUYA SAITO[2], AND TOMOYUKI UENO[2]

[1]Graduate School of Environmental, Life, Natural Science and Technology, Okayama University, Kita-ku, Okayama 700-8530, Japan
[2]Sumitomo Electric Industries Ltd., Itami, Hyogo 664-0016, Japan

Corresponding author: Ren Tsunata (tsunata@okayama-u.ac.jp)

ABSTRACT This study aims to improve the torque performance and manufacturability of axial-flux permanent magnet (AFPM) machines. Hence, we propose a novel AFPM machine that employs a soft magnetic composite (SMC) core with tooth-tips constructed by a one-pressing process and die. In this paper, the proposed AFPM machine is compared to two conventional AFPM machines using an SMC core. One of them has open-slot structure without tooth-tips. Another model employs an SMC core with tooth-tips pressed by a conventional pressing process that requires multiple operations and dies. As a result of the comparison, the proposed AFPM machine realizes a much higher torque than the two conventional machines. Additionally, the manufacturability of an SMC core with tooth-tips pressed by the proposed method is superior to the conventional one because the proposed structure can be realized by the one-pressing process and die. Furthermore, two prototypes of the proposed AFPM machine and the conventional one with an open-slot structure are fabricated, and then, they are compared by experiments. Consequently, the proposed AFPM machine achieves a 15.7% higher torque than that of the conventional machine using an open-slot structure. Finally, this paper presents an improved design of an AFPM machine with SMC cores using the proposed pressing process. As a result, the proposed AFPM realizes a 20% larger torque than that of a conventional model employing an open-slot structure.

INDEX TERMS Axial-flux permanent magnet machine, soft magnetic composite (SMC), PMSM, tooth-tips, torque, press process, semi-closed slot structure, axial gap motor, mass production, YASA motor, shoe.

I. INTRODUCTION

Axial-flux permanent magnet (AFPM) machines have been recently gaining attention because of their high torque density. Many research groups have been developing AFPM machines for various applications for decades, and these research results have shown the superiority of AFPM machines to radial-flux permanent magnet (RFPM) machines in various cases. Compared to an RFPM machine, an AFPM machine has 24.8% higher torque density [1]. In [2], an AFPM machine achieves higher efficiency than that of an RFPM machine by employing a neodymium-bonded permanent magnet (Nd-bonded PM) while maintaining a higher torque. Additionally, the temperature rise of an AFPM is 26.4% lower than that of an RFPM machine under the same volume and operating conditions [3].

One effective method for enhancing the torque performance of AFPM machines is to employ tooth-tips for the stator core [4], [5], [6]. However, it is normally difficult to construct the tooth-tips for AFPM machines because

The associate editor coordinating the review of this manuscript and approving it for publication was Feifei Bu.

they have a three-dimensional shape. The stator core with tooth-tips of AFPM machines can be realized using a radially laminated steel sheet [7], but its manufacturing cost is extremely high. In [8], an AFPM machine with tooth-tips using the additive manufacturing by 3D-Printer is proposed. However, the research does not include experimental verification. On the other hand, the stator core with tooth-tips made of soft magnetic composite (SMC) can be manufactured owing to its magnetic isotropy [9]. However, the tooth-tips need to be separately manufactured from other components such as the back yoke in the conventional manufacturing method, and therefore, several dies are required to press all parts and additional processes to adhere them [10], [11]. In other words, the SMC core with tooth-tips pressed by the conventional process is not suitable for mass production due to high manufacturing cost. In addition, since tooth-tips have a very thin structure, it is difficult to press them alone, resulting in poor manufacturability. Accordingly, it is desirable to construct an SMC core with tooth-tips using a one-pressing process and die.

Yokeless and segmented armature (YASA) machine is one of the AFPM machines in which the tooth-tips are frequently used [12], [13]. The thickness of the tooth-tips in many YASA machines is large because they are large size. Therefore, the tooth-tips can be realized by one-press process. As a result, it is possible to separate the tooth-tips and teeth, and glue them together. However, since target of this paper is small-size AFPM machines for industrial applications, the problems described above occur.

This paper proposes an SMC core with tooth-tips constructed by a one-pressing process to enhance the torque performance and manufacturability of small-size AFPM machines at the same time. The proposed AFPM machine can simultaneously realize high torque and high manufacturability. In this paper, the proposed AFPM machine is compared to two conventional AFPM machines using an SMC core. A conventional AFPM machine has an open-slot structure without tooth-tips. Another conventional model employs tooth-tips constructed using a conventional pressing process.

The remainder of this paper is organized as follows. In Section II, the structures of the proposed and two conventional AFPM machines are presented. Additionally, the superiority and details of the proposed one-pressing method and the AFPM machine employing it are described. Section III presents the simulation results of the three AFPM machines obtained by three-dimensional finite element analysis (3D-FEA), and then, the torque and efficiency are compared. In Section IV, two prototypes of the proposed AFPM machine and the conventional machine employing the open-slot structure are evaluated and compared experimentally. Finally, this paper presents an improved design of an AFPM with SMC cores using the proposed pressing process in Section V. Section VI concludes this paper.

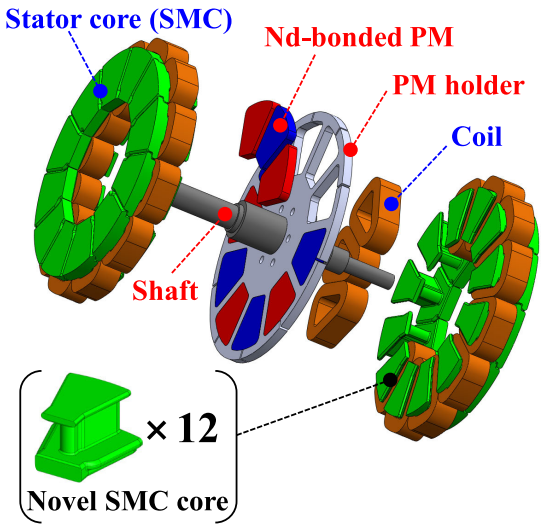

FIGURE 1. Exploded view of proposed AFPM machine employing SMC core with tooth-tips constructed by one pressing process.

II. STRUCTURE AND PRESSING PROCESS OF CONVENTIONAL AND PROPOSED AFPM MACHINES

A. PROPOSED PRESSING METHODS AND PROCESS

Fig. 1 shows an exploded view of the proposed AFPM machine employing an SMC stator core constructed using a novel one-pressing process. The proposed AFPM machine employs the fractional-slot (10 poles / 12 slots) combination to reduce torque ripple [14]. Therefore, one side stator core with tooth-tips is composed of 12 pieces of SMC cores. Additionally, the proposed AFPM machines use a double-stator and single-rotor structure [15]. Fig. 2 shows a real SMC core with a tooth-tip constructed by the proposed one-pressing operation and die. This SMC core with tooth-tips is pressed in the radial direction, and hence, the tooth-tip, tooth and back yoke can be simultaneously constructed by one pressing process and die. The magnetic and mechanical properties of SMC vary with the pressing pressure [16]. Therefore, the SMC core shown in Fig. 2 was properly pressed using a suitable pressure to construct it. The proposed SMC core with a tooth-tip has sufficient feasibility from the perspective of the dimensions. In the proposed pressing method, the SMC core is not de-burred after pressing. The burr does not appear because the adequate clearance is employed in the proposed pressing method. In addition, a special coating on the die suppresses the increase in the eddy current loss in the SMC core. The shiny surfaces of the SMC core shown in Fig. 2 are traces of sliding when ejecting from the die.

Fig. 3 shows the stator cores of the three comparative AFPM machines. Additionally, Fig. 4 illustrates the pressing process and dies in each AFPM machine. In all models, the total height of the stator core is constant at 17.8 mm. Model-A, shown in Fig. 3(a), is a conventional model using the open-slot structure without tooth-tips; and therefore, the

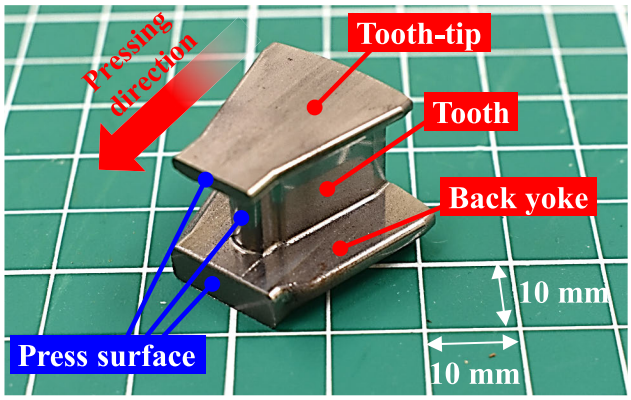

FIGURE 2. Real SMC core having tooth-tip constructed by proposed one pressing process and die.

slot opening width w_s is the largest of them [2]. Consequently, the area facing the air gap is the smallest of 165 mm^2. As shown in Fig. 4(a), the SMC core for the open-slot structure is normally pressed in the axial direction. Moreover, the SMC core of Model-A can be constructed by one pressing process and die, but the torque performance cannot be enhanced because it does not have tooth-tips. In addition, in Model-A, two teeth are pressed in one step because magnetic resistance can decrease by reducing the number of air gap. However, as the number of teeth extremely increases, larger press force is required. This means that the size of press machine becomes dramatically larger. Large press machine and dies not desirable from perspective of equipment cost.

Fig. 3(b) shows Model-B, which employs a semi-closed slot structure. Model-B's SMC core with the tooth-tips is constructed by a conventional method that requires multi-pressing process and dies [17]. Fig. 4(b) shows the conventional pressing process for Model-B. In the conventional process, the tooth-tips need to be separately pressed from other parts, such as the back yoke and the tooth. This implies that two different dies and two pressing operations are required, and the manufacturing cost increases. Additionally, pressing the tooth-tips is basically difficult because its axial thickness is very thin. Furthermore, the process of bonding the two parts by adhesive and adjusting the position of the tooth-tips are also required after pressing. Thus, the conventional pressing process for Model-B is unsuitable for mass production.

Fig. 3(c) shows Model-C proposed in this paper. Model-C is a semi-closed structure with tooth-tips; however, the pressing process and direction are different from those of Model-B. All parts of the SMC core in Model-C are simultaneously pressed in the radial direction by a single die. Additionally, the radial thickness of the tooth-tips is not thin, which improves manufacturability. Fig. 4(c) shows a schematic of the proposed one-pressing process that can construct tooth-tips with other parts at the same time. The slot opening width w_s of Model-C is set to 6.2 mm which is the same as that of Model-B. On the other hand, the SMC core of Model-C has

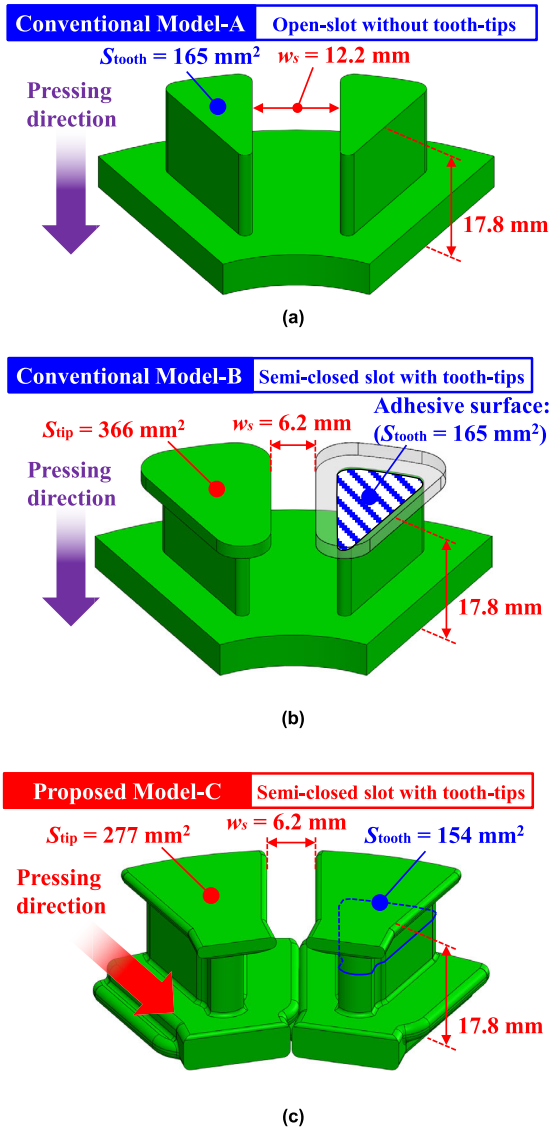

FIGURE 3. SMC core in three comparative models of AFPM machines. (a) Model-A having conventional open-slot structure. (b) Model-B having tooth-tips constructed by conventional pressing method. (c) Model-C having tooth-tips constructed by proposed one pressing process.

a suitable shape for the radial pressing direction, and resultantly, the area facing the air gap S_{tip} and the cross-sectional area of tooth S_{tooth} are 24.3% and 6.7% smaller than those of Model-B, respectively. Additionally, as shown in Fig. 4(c), the radial length of tooth-tips and back yoke can be adjusted in the proposed pressing method. For example, the SMC core of Pattern-2 in Fig. 4(c) has overhang tooth-tip and back yoke in the radial direction. This means that the shape of tooth-tips and back yoke can be adjusted depending on the AFPM design.

Fig. 5 shows mechanical constraints of pressed SMC core for Model-C in the proposed one-pressing method. In the proposed one-pressing method, the linear parts should be employed for the SMC core in the pressed direction, as shown in Fig. 5. The proposed shape of SMC core achieves both

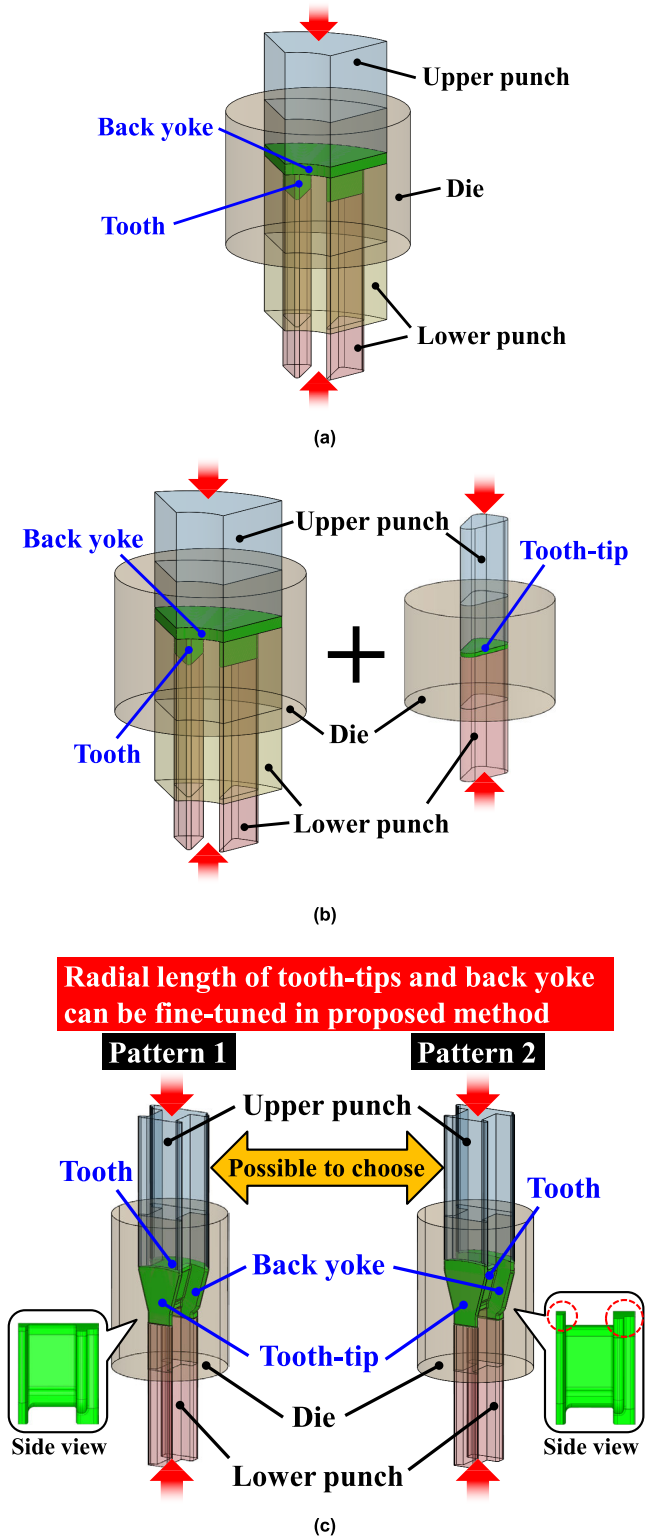

FIGURE 4. Schematic of pressing process and dies for each model. (a) Model-A. (b) Model- B. (c) Proposed Model-C.

high electromagnetic performances and manufacturability, considering the mechanical constraints. The maximum pressure is different depending on parts of the SMC core in

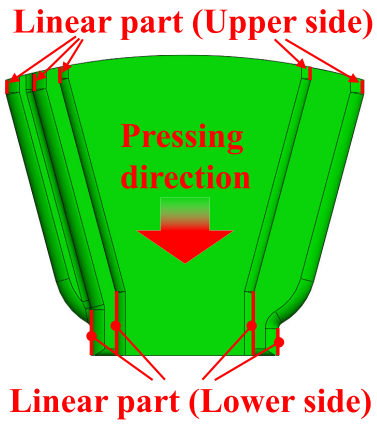

FIGURE 5. Mechanical constraints of pressed SMC core for Model-C.

TABLE 1. Parameters regarding winding of three comparative models.

Item	Model-A	Model-B	Model-C
Coil space factor	40%	40%	40%
Coil space area Sc	72.6 mm^2	63.1 mm^2	69.4 mm^2
No. of turns	46 turn/slot	40 turn/slot	44 turn/slot
Resistance	0.95 ohm	0.83 ohm	0.86 ohm

Model-C. This is because the length of each part is different in the pressing direction. As a result, the maximum pressure in the tooth-tips and tooth are approximately 800 MPa and 1000 MPa, respectively. Accordingly, the mass density in the tooth-tips is slightly different from tooth due to the different pressure. However, in the proposed method, the SMC core is pressed and formed so that the average density matches the design value. Therefore, although there is a possibility that the design value and the actual value may deviate locally, the overall SMC core is manufactured so that the deviation is minimized.

Fig. 6 shows two AFPM machines that employ SMC cores fabricated by the proposed one-pressing process. The two AFPM machines have the same rotor structure. In Fig. 6(a), the outer diameter of the PMs and tooth-tips are identical. In contrast, the AFPM machine shown in Fig. 6(b) has radially larger tooth-tips than the PMs. The portion of tooth-tips that is radially larger than PM does not contribute to the improvement of the average torque. Accordingly, the AFPM machine shown in Fig. 6(a) is chosen as Model-C in this case, although the SMC core shown in Fig. 6(b) can be manufactured using the proposed pressing method.

Fig. 7 shows the winding process for the mass production of Model-C. First, the nozzle winds a copper wire around the SMC cores with tooth-tips arranged in a straight line. Second, each phase coil is continuously wound, and the coils are set to all SMC cores. In this case, the coil space factor can be maintained high because the distance between the SMC cores is larger than the nozzle. Additionally, the copper wire can be

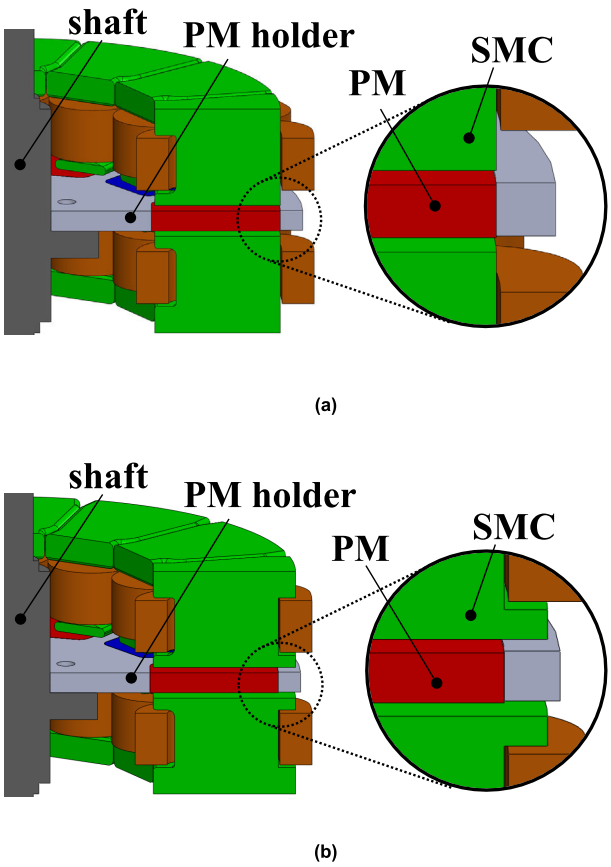

FIGURE 6. Stator core variations and AFPM models that can be realized by proposed method. (a) Without outer radial tooth-tips and yoke (Model-C). (b) With outer radial tooth-tip and yoke.

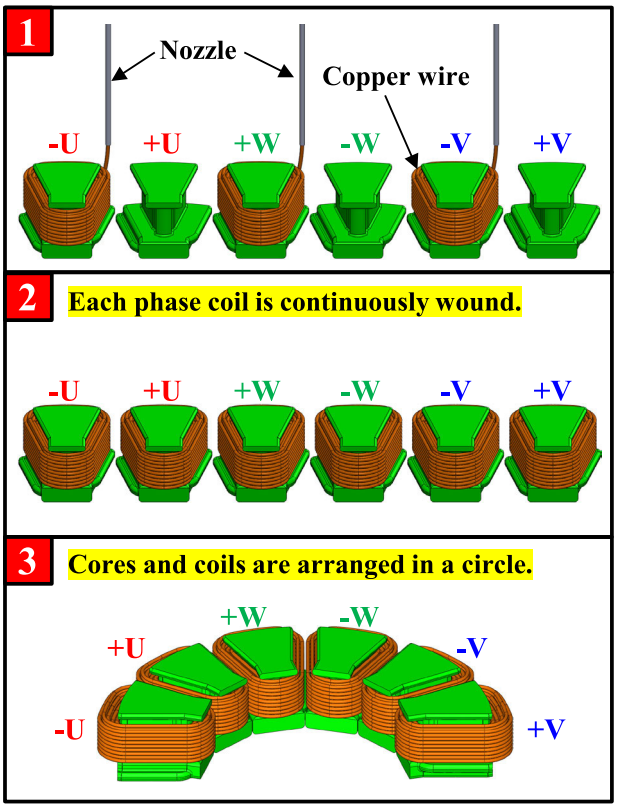

FIGURE 7. Winding process in mass production of proposed Model-C with SMC core manufactured one-pressing method.

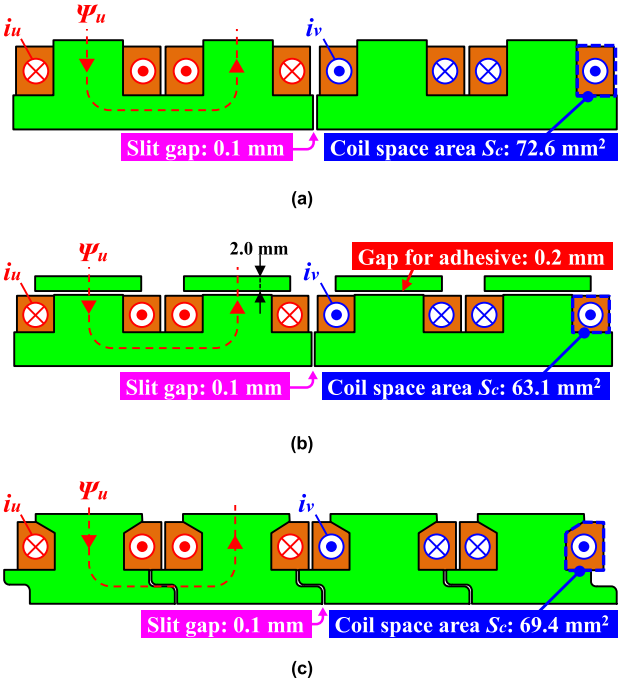

FIGURE 8. Magnetic path and gaps in stator cores. (a) Model-A. (b) Model-B. (c) Proposed Model-C.

wound directly on the SMC core because the tension from the winding can be received by the tooth-tips in Model-C. Finally, all the cores and coils are arranged in a circle to complete the stator. On the other hand, in Model-A employing the open-slot structure, a bobbin is required to wind the copper wire around the SMC core. Model-B also needs a bobbin because tooth-tips are bonded after winding the copper wire. Model-C can choose bobbin or insulating paper depending on the application and manufacturing facilities, achieving higher manufacturability. Additionally, in Model-A, an air-core coil including a bobbin is fabricated and inserted into the SMC core because it has an open slot structure. Model-C winds the coil directly on the SMC core as shown in Fig. 7. In both cases, the winding time is almost the same. In addition, Model-C does not require the process of inserting an air-core coil to the SMC core, so it is possible to reduce costs.

Fig. 8 describes the magnetic path, gaps, and coil space area S_c in the stator core for the three models. In Model-A, each SMC core has two teeth pressed by one die; and therefore, there is no slit gap in the magnetic path of the U-phase current i_u. Whereas in Model-B, the magnetic path of the U-phase flux generated by an armature current has two gaps for adhesive of 0.2 mm, causing a reduction in the average torque. Additionally, in Model-B, the tooth-tips are bonded to the teeth after the coils are wound. Consequently, the coil space area S_c of Model-B is the smallest of them.

TABLE 2. Dimensions and operating condition.

Parameter	Value
Outer diameter	110 mm
Axial length	41.3 mm
Air gap length	1.0 mm
PM thickness	3.7 mm
Number of poles/slots	10 poles/12 slots
Coil space factor	40%
DC-bus voltage	282V
Rated current density	4.0 Arms/mm^2
Rotational speed	1000 rpm

Additionally, the thickness of tooth-tips in Model-B is set to 2 mm, which is the minimum thickness that can be pressed, but the coil space area S_c in Model-B is reduced owing to it. In contrast, Model-C has 10% larger coil space area S_c than Model-B because the coils can be directly wound to the SMC core. Moreover, Model-C has fewer gaps than Model-B because Model-C does not have gaps for adhesive between the tooth-tips and tooth.

Table 1 lists winding parameters of three comparative models. The coil space factor is constant at 40% in all models, for better comparison. However, as mentioned the above, the coil space area S_c is different, and Mode-B has the smallest value due to the tooth-tips pressed by the conventional method. Consequently, the number of turns and resistance of Model-B are also the smallest of them. Model-C has larger electromagnetic force than Model-B because of larger number of turns. Model-A has the largest coil space area S_c of them, but it does not have the tooth-tips, and hence, it cannot effectively use the magnetic flux generated by permanent magnets (PMs).

B. PARAMETERS AND MATERIALS

Table 2 shows dimensions and operating conditions of three comparative models. All models have same total axial length and outer diameter (namely same motor volume). The inner diameter of Model-A and -B is 40.8 mm. In Model-C, the inner diameter is determined by the shape of die and lower punch, resulting in 53 mm which is larger than Model-A and Model-B. They employ same rotor structure, as shown in Fig. 9. In other words, the only difference between them is stator structure, for better comparison. The rated current density of the three models is set to 4.0 Arms/mm^2 because they can continuously operate without cooling [3].

Table 3 lists materials used for three models. The SMC chosen for the stator core has a good iron loss property (HB2, Sumitomo Electric Industries, Ltd.) [18]. All models employ Nd-bonded PM (S5B-17ME, Aichi Steel Co. Ltd.), which has an extremely low conductivity (14.3 S/m), restraining the eddy current loss within it [19]. The residual magnetic flux density B_r and the coercive force H_c of Nd-bonded PM are 0.81 T and 473 kA/m, respectively.

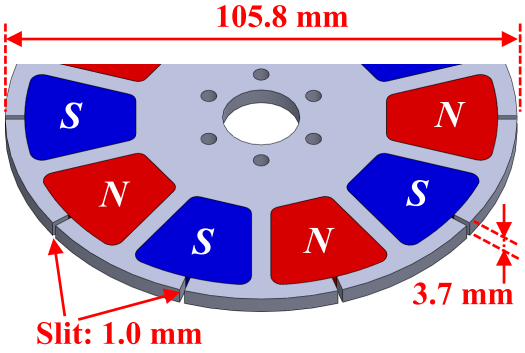

FIGURE 9. Coreless rotor structure for three AFPM machines.

TABLE 3. Materials used for three comparative models.

Part	Material	Model No.
Stator core	Soft magnetic composite	HB2
Coil	Copper	-
PM	Nd-bonded PM	S5B-17ME
PM holder	Non-magnetic stainless	SUS304

Nd-bonded PMs are held by non-magnetic stainless PM holder (SUS304), and hence, the rotor does not have magnetic core. This rotor structure is therefore referred as a coreless rotor structure. Fig. 9 shows the coreless rotor structure of the three comparative AFPM machines. The thickness of the Nd-bonded PMs and PM holder are the same. The coreless rotor has 1.0 mm slit on its outside because the eddy current loss in the PM holder can be reduced [20].

Fig. 10 shows the measured magnetic properties of the SMC (HB2) material used for the three AFPM machines. Fig. 10(a) shows an experimental sample of SMC used to measure the B-H characteristics and iron loss. Figs. 10(b) and (c) show the B-H curve and iron loss density of HB2. HB2 has good magnetic properties because its magnetic permeability and iron loss density are almost the same as those of an electromagnetic steel sheet (35A360) [18].

III. 3D-FEA RESULTS OF THREE COMPARATIVE AFPM MACHINES

Fig. 11 shows the magnetic flux density distributions in the stator cores of three comparative AFPM machines under rated operating conditions (1000 rpm, 4.0 Arms/mm^2). The overall magnetic flux densities in the three models are not very high because the magnetic resistance is high owing to its coreless rotor structure. This means that the three models could be smaller size. On the other hand, in this paper, the comparison is performed under the condition that the teeth

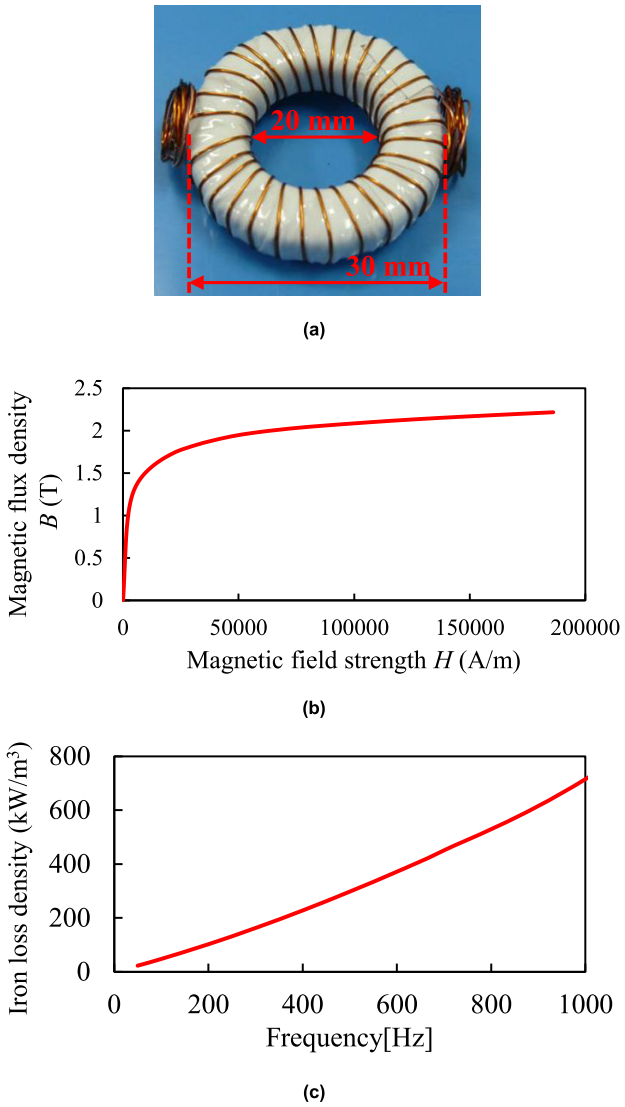

FIGURE 10. Magnetic properties of SMC (HB2). (a) Experimental sample of SMC. (b) B-H characteristic. (c) Iron loss density.

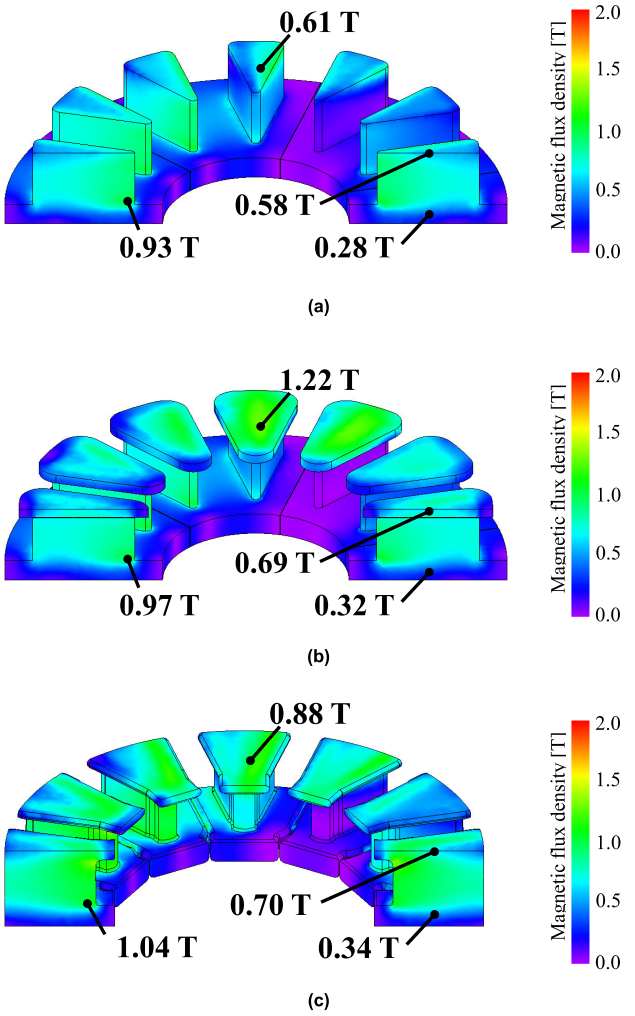

FIGURE 11. Magnetic flux density distributions in SMC stator cores of three comparative AFPM machines at 1000 rpm and 4.0 Arms/mm ^{2}. (a) Mode-A. (b) Model-B. (c) Proposed Model-C.

are not magnetically saturated, and hence, the effect of the tooth-tips can be clearly evaluated.

In Model-A, the maximum magnetic flux density is the lowest of all models because the magnetic flux generated by PMs is not effectively used due to the open-slot structure without tooth-tips. On the other hand, Model-B, which has conventional tooth-tips, has the highest maximum magnetic flux density. The magnetic flux density in the tooth-tips of Model-B is especially high because of the slit gap for adhesive between tooth-tips and teeth. However, the magnetic flux density in the teeth and back yoke is not higher than that in Model-C. This means that the magnetic flux contributing to the generation of torque in Model-B is less than that in Model-C. In contrast, the magnetic flux density in the tooth-tips of Model-C is lower than that of Model-B because its SMC core does not have a slit gap between tooth-tips and teeth because of the proposed integrated core. However, Model-C can effectively use the magnetic flux obtained by the PMs to generate torque, as mentioned above. While Model-B and Model-C having the tooth-tips can effectively use magnetic flux generated by PMs, and it can be predicted that iron loss becomes larger than that of Model-A without tooth-tips because the magnetic flux density in the tooth-tips is relatively high.

Furthermore, Fig. 12 shows the iron loss density distributions in the stator cores of the three comparative AFPM machines under the same operating conditions as those in Fig. 11. The iron loss density in Model-A is overall low because the magnetic flux density is low. In Model-B and Model-C, the iron loss density in tooth-tips is higher compared to other parts of the stator.

In AFPM machines, axial magnetic force normally occurs in the stator core; therefore, the stator core needs to be properly fixed [21], [22], [23]. In particular, tooth-tips need to be bonded to the teeth in Model-B because they are separated. Fig. 13 shows a 3D-FEA result of axial force F_z in the

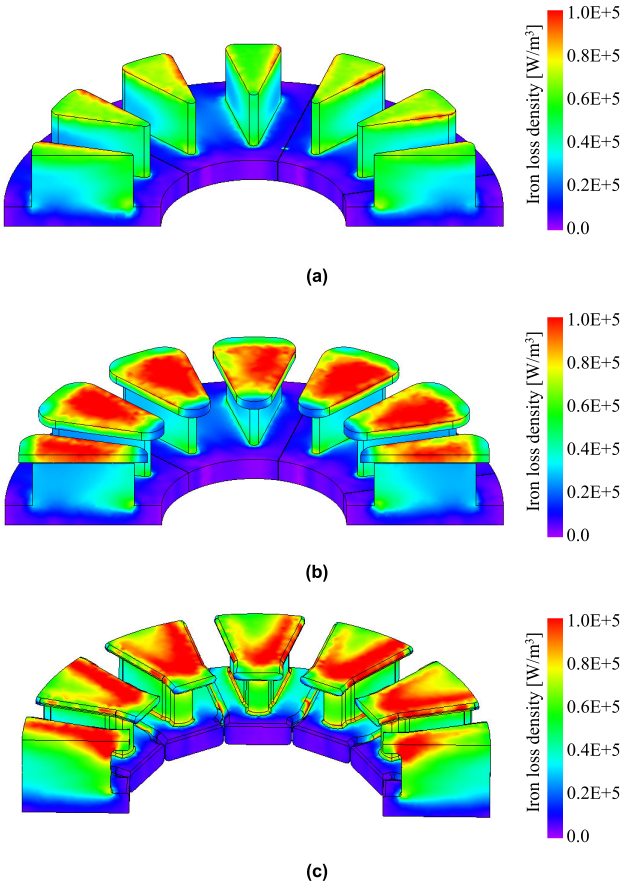

FIGURE 12. Iron loss density distributions in SMC stator cores of three comparative AFPM machines at 1000 rpm and 4.0 Arms/mm2. (a) Mode-A. (b) Model-B. (c) Proposed Model-C.

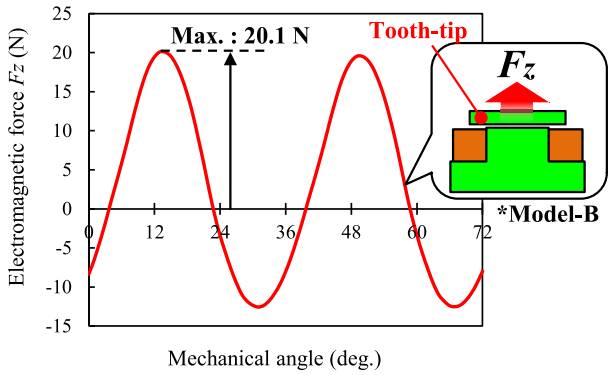

FIGURE 13. Axial magnetic force F_z in tooth-tips of conventional Model-B at 1000 rpm, 4.0 Arms/mm^2.

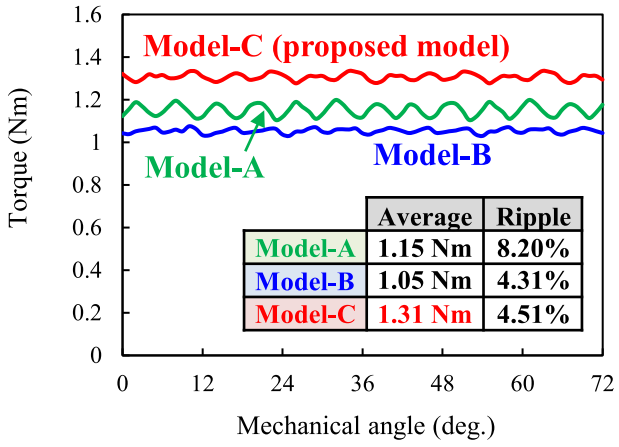

FIGURE 14. Torque waveforms of three comparative AFPM machines at 1000 rpm, 4.0 Arms/mm^2.

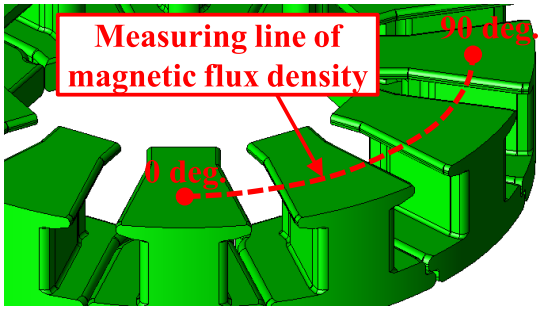

FIGURE 15. Measuring line of magnetic flux density in the air gap.

tooth-tip of conventional Model-B under rated operating conditions (1000 rpm, 4.0 Arms/mm^2). The maximum axial force in tooth-tips is 20.1 N, and the adhesive must be provided to withstand this force. If PMs with higher residual magnetic flux density (e.g., Nd-sintered PM) than Nd-bonded PM are used for AFPM machines, fixing tooth-tips becomes more difficult due to large axial force. Additionally, Model-B's manufacturability is also not good because it is not easy to decide the tooth-tips position accurately in the manufacturing process.

Fig. 14 shows the torque waveforms of three comparative AFPM machines under rated operating conditions (1000 rpm, 4.0 Arms/mm^2). The average torque of Model-B is the smallest, although tooth-tips are employed. This is because the electromagnetic force caused by winding is the smallest owing to the fewer number of turns and smaller coil space area S_c of Model-B. Model-A, which employs the open-slot structure, has a middle characteristic in terms of the average torque, but the torque ripple is the largest. In contrast, the proposed Model-C realizes the largest average torque which is 14% higher than that of Model-A. Additionally, Model-B and Model-C have lower torque ripples than Model-A because the tooth-tips are employed. Consequently, Model-C with tooth-tips pressed by the proposed method can simultaneously realize a large torque and low torque ripple.

Fig. 15 shows measuring line of the magnetic flux density in the air gap. The measuring line is in the middle of the air gap in the axial direction. Additionally, the radius of the measuring line is 40 mm. Fig. 16 shows the magnetic flux density waveforms and harmonic spectrum of the three models. All models have the low-order harmonics because they employ the fractional-slot combination (10 pole / 12 slots). According

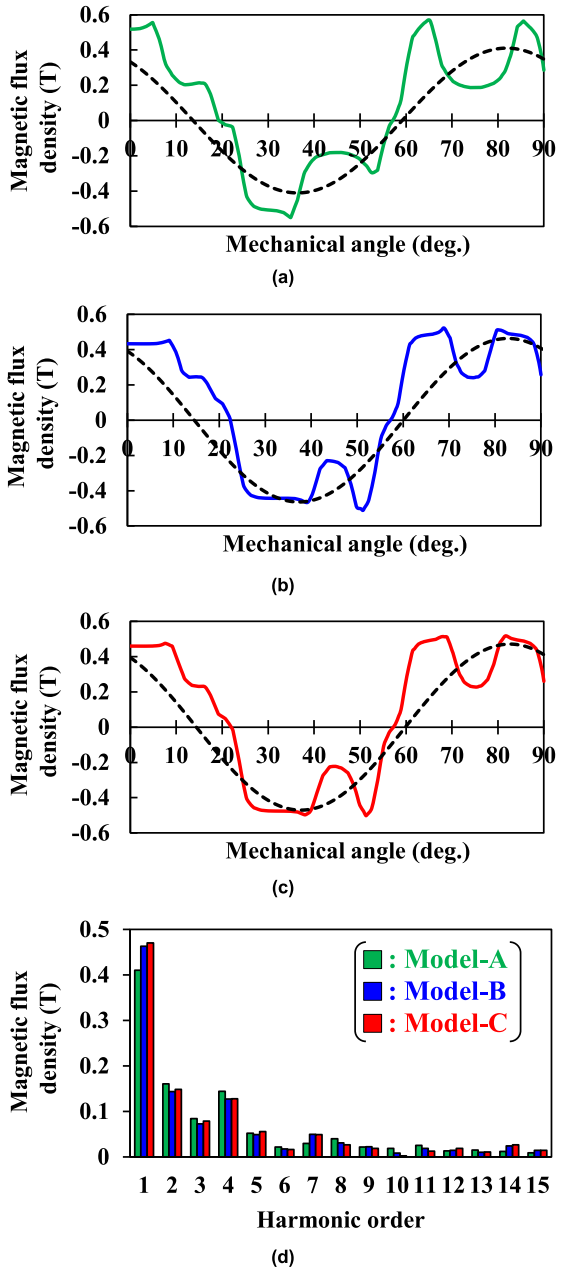

FIGURE 16. Magnetic flux density waveforms and harmonic spectrum of three AFPM machines under no-load condition. (a) Model-A. (b) Model-B. (c) Model-C. (d) Harmonic spectrum.

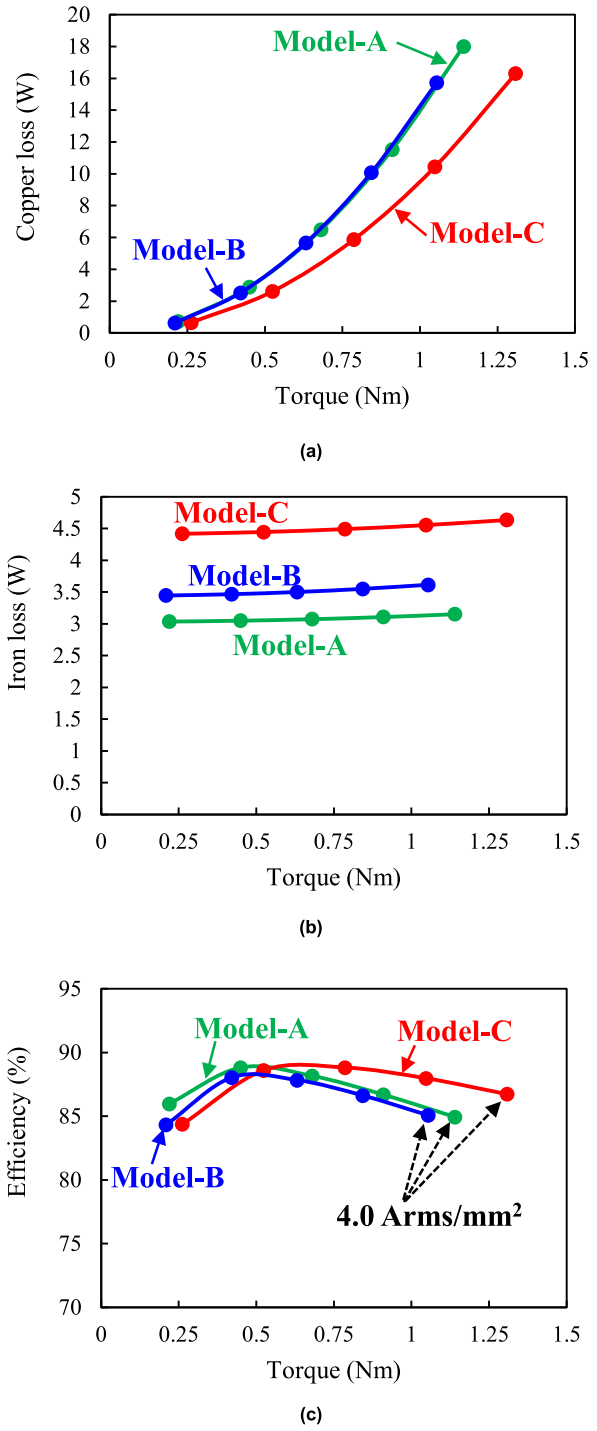

FIGURE 17. Loss and efficiency versus torque of three comparative AFPM machines at 1000 rpm. (a) Copper loss. (b) Iron loss. (c) Efficiency.

to Fig. 16(d), the fundamental component of the proposed Model-C is the largest of them, resulting in the largest average torque, as shown in Fig. 14. In contrast, Model-A has the smallest fundamental magnetic flux density of them although its average torque is larger than that of Model-B. This is because Model-B has fewer winding turns than Model-C, as shown in Table 1. In other words, Model-B has the smallest average torque of them due to the inadequate coil space area.

Fig. 17 compares the copper loss, iron loss, and efficiency of the three AFPM machines at 1000 rpm. The copper loss of the proposed Model-C is the smallest over a wide operating range because of its good torque performance, as shown in Fig. 17(a). However, as shown in Fig. 17(b), the iron loss in Model-C is the largest owing to the high magnetic flux density in the teeth and back yoke. However, the efficiency of Model-C is the highest in most of the operating torque areas because copper loss is dominant in this operating area.

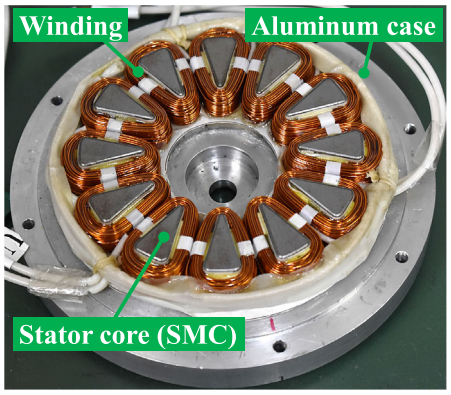

(a)

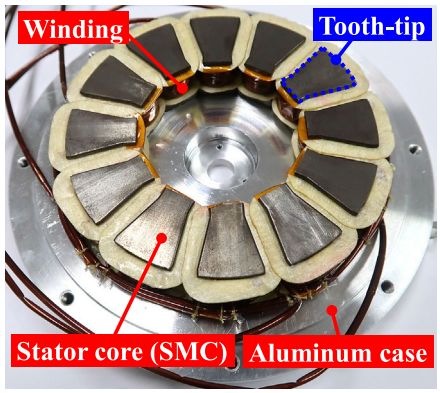

(b)

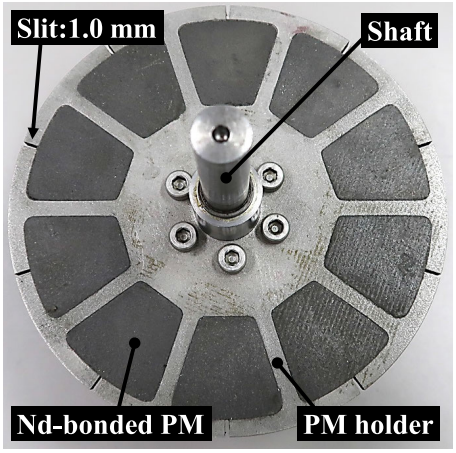

(c)

FIGURE 18. Prototypes of Model-A and Model-C. (a) Stator of Model-A without tooth-tips. (b) Stator of Model-C using tooth-tips pressed by proposed method. (c) Rotor used in two prototypes.

Moreover, as the torque increases, the difference in efficiency between Model-C and the other models gets larger.

IV. EXPERIMENTAL RESULTS OF CONVENTIONAL MODEL-A AND PROPOSED MODEL-C

In this section, the proposed Model-C, which realizes high torque and efficiency performance, is evaluated experimentally. Additionally, Model-C is compared to Model-A, which

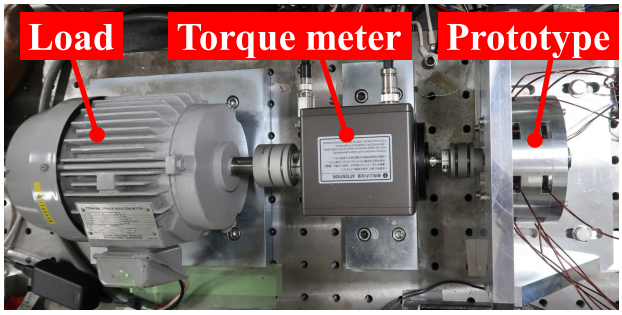

FIGURE 19. Test platform for experiments.

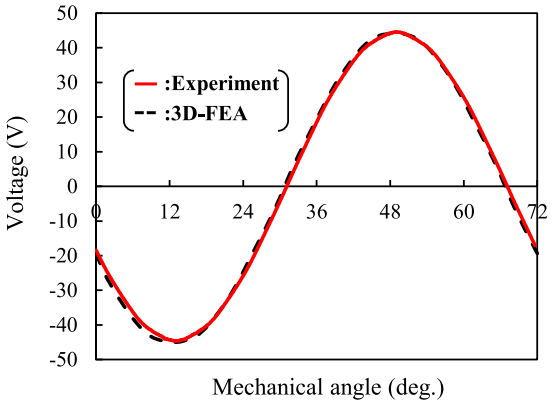

FIGURE 20. Comparison of measured and FEA-predicted back-EMF of proposed Model-C at 1000 rpm.

employs the open-slot structure, in the experiments. Fig. 18 shows the prototypes of Model-A and Model-C. The SMC cores for the two prototypes are fabricated by presswork. The two prototypes have the same two stators because they employ the double-stator and single-rotor structure. In both machines, the SMC cores are fixed to an aluminum case using an adhesive. Both machines use the same coreless rotor, as shown in Fig. 18(c). The coreless rotor has Nd-bonded PMs and 1.0 mm slits. Fig. 19 shows the platform for the experiments for the two prototypes.

Fig. 20 shows the measured and FEA-predicted back-EMF waveforms of the proposed Model-C with tooth-tips at 1000 rpm under no-load conditions. The measured and FEA-predicted values are in good agreement, indicating that the prototype is manufactured with a high accuracy. Fig. 21 shows the measured and FEA-predicted average torques versus current density in Model-A and Model-C at 1000 rpm. In both machines, the measured torque is in very good agreement with the 3D-FEA results. Additionally, the proposed Model-C obviously has better torque performance than the conventional Model-A without tooth-tips. Consequently, Model-C can realize 15.7% higher average torque than Model-A at the rated current density. Accordingly, the tooth-tips constructed by the proposed one-pressing process can contribute to enhancing the torque performance and efficiency of AFPM machines while maintaining the high

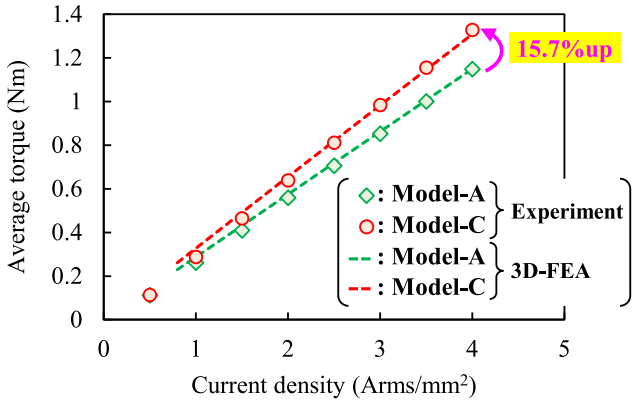

FIGURE 21. Comparison of measured and FEA-predicted torque versus current density characteristics between in both machines at 1000 rpm.

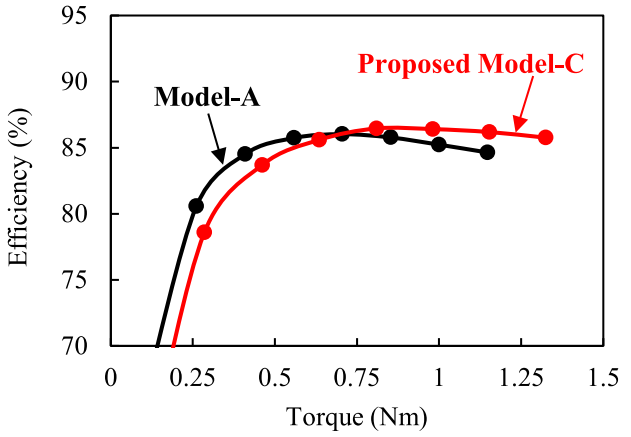

FIGURE 22. Measured efficiency versus torque of both machines at 1000 rpm.

manufacturability of SMC. Fig. 22 shows the efficiency of both the prototypes at 1000 rpm. Similar to the FEA-predicted results shown in Fig. 17(c), the proposed Model-C indicates higher torque and efficiency Model-A in the -torque region.

V. INVESTIGATION INTO FURTHER IMPROVEMENT OF TORQUE PROPERTIES BY PROPOSED METHOD

As show in Fig. 4(c), in the proposed one-pressing method, the shape of tooth-tips and back yoke can be adjusted in the radial direction depending on the AFPM design. This section presents a better design of the AFPM machine to enhance the average torque within the same motor volume.

Fig. 23 shows the rotor change to improve the average torque. The outer diameter of the modified rotor is the same as that of the stator. As a result, outer radius of PMs increases from 48.9 mm to 52 mm. In the modified rotor, the mechanical strength is considered at the maximum rotational speed of 1000 rpm. Fig. 24 shows two AFPM machines that employ the modified rotor. Fig. 24(a) is Model-A-2, which combines the open-slot structure with the modified rotor. The stator shape of Model-A-2 is the same as that of Model-A.

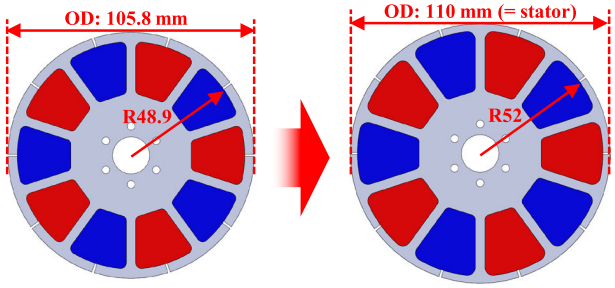

FIGURE 23. Rotor changes for higher torque model (Model-D).

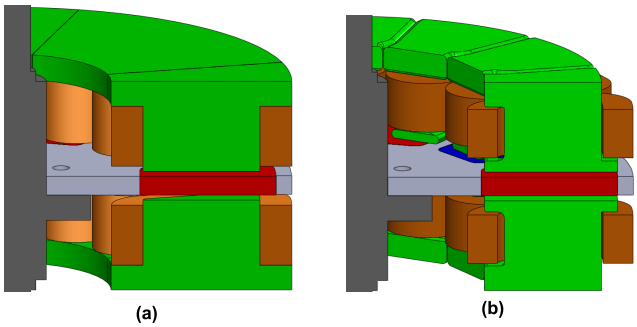

FIGURE 24. Cross-sectional views of two comparative models. (a) Model-A-2 combining open-slot structure with a modified rotor. (b) Model-D employing outer radial tooth-tips and a modified rotor.

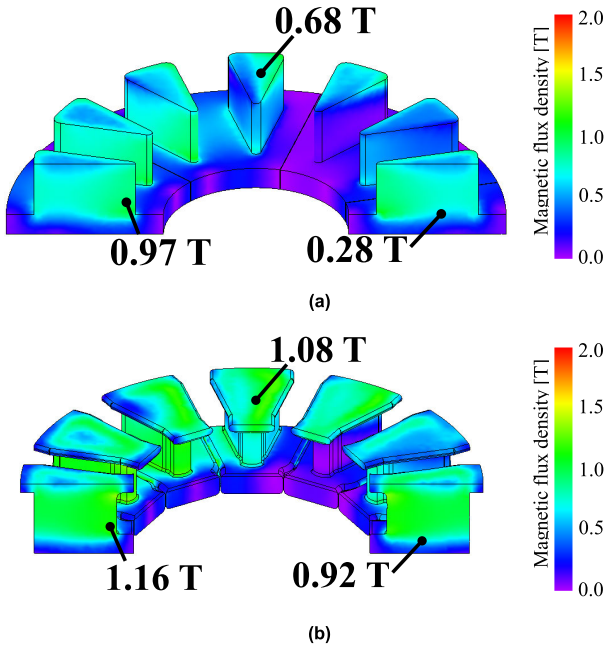

FIGURE 25. Magnetic flux density distributions in SMC stator cores of two comparative AFPM machines employing a modified rotor at 1000 rpm and 4.0 Arms/mm^2. (a) Mode-A-2. (b) Model-D.

Fig. 24(b) shows the proposed Model-D combining the SMC stator with tooth-tips largened in the radial direction and the modified rotor. In Model-D, as the PM radius increases,

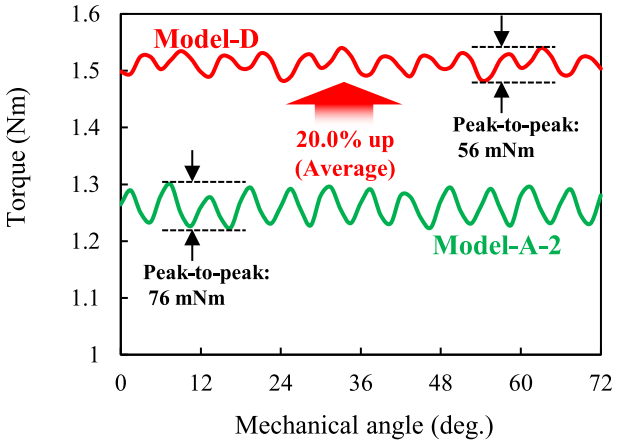

FIGURE 26. Torque waveforms of Model-A-2 and Model-D at 1000 rpm, 4.0 Arms/mm^2.

the tooth-tips radius also increases, resulting in the same radius each other.

Fig. 25 shows the magnetic flux density distributions of Model-A-2 and the proposed Model-D under the same current density conditions. The magnetic flux density of Model-D is much higher than that of Model-A-2 because Model-D can effectively use the increased magnetic flux caused by the modified rotor. In other words, Model-A-2 is not able to effectively use the increased magnetic flux of the modified rotor owing to the open-slot structure.

Fig. 26 shows the torque waveforms of Model-A-2 and Model-D at 1000 rpm and 4.0 Arms/mm^2. Model-D realizes 20.0% larger average torque than that of Model-A-2. This difference is larger than that between Model-A and Model-C, as shown in Fig. 14. This means that the outer diameter side is especially useful for increasing the surface area of the PMs, resulting in a larger magnetic flux. Furthermore, the peak-to-peak value of the torque in Model-D is 26.3% smaller than that of Model-A-2. Accordingly, the torque characteristics of an AFPM machine can be enhanced by the proposed method depending on the application and cost.

VI. CONCLUSION

This paper proposed an SMC core with tooth-tips constructed by a one-pressing process to enhance the torque performance and manufacturability of small-size AFPM machines at the same time. An AFPM machine employing an SMC core with tooth-tips constructed by the proposed one-pressing process is evaluated by 3D-FEA and experiment, and resultantly, the proposed machine realizes 15.7% higher torque than that of the conventional machine using an open-slot structure without tooth-tips. Moreover, the manufacturability of the proposed AFPM machine is improved, compared with the conventional machine that employs separated tooth-tips. Additionally, this paper presents an example that explains the improved design of an AFPM machine to enhance torque characteristics using the proposed pressing method. Consequently, the proposed AFPM machine achieves high torque, efficiency, and low torque ripple simultaneously. The SMC core with tooth-tips constructed by the proposed one-pressing process is very effective in improving the torque performance of AFPM machines while maintaining manufacturability.

REFERENCES

[1] L. Li, W. N. Fu, S. L. Ho, S. Niu, and Y. Li, "A quantitative comparison study of power-electronic-driven flux-modulated machines using magnetic field and thermal field co-simulation," *IEEE Trans. Ind. Electron.*, vol. 62, no. 10, pp. 6076–6084, Oct. 2015.

[2] R. Tsunata, M. Takemoto, S. Ogasawara, A. Watanabe, T. Ueno, and K. Yamada, "Development and evaluation of an axial gap motor using neodymium bonded magnet," *IEEE Trans. Ind. Appl.*, vol. 54, no. 1, pp. 254–262, Jan. 2018, doi: 10.1109/TIA.2017.2710123.

[3] R. Tsunata, M. Takemoto, J. Imai, T. Saito, and T. Ueno, "Comparison of thermal characteristics in various aspect ratios for radial-flux and axial-flux permanent magnet machines," *IEEE Trans. Ind. Appl.*, vol. 59, no. 3, pp. 3353–3367, Jun. 2023, doi: 10.1109/TIA.2023.3255845.

[4] G. D. Donato, F. G. Capponi, and F. Caricchi, "On the use of magnetic wedges in axial flux permanent magnet machines," *IEEE Trans. Ind. Electron.*, vol. 60, no. 11, pp. 4831–4840, Nov. 2013.

[5] V. Simón-Sempere, A. Simón-Gómez, M. Burgos-Payán, and J.-R. Cerquides-Bueno, "Optimisation of magnet shape for cogging torque reduction in axial-flux permanent-magnet motors," *IEEE Trans. Energy Convers.*, vol. 36, no. 4, pp. 2825–2838, Dec. 2021.

[6] M. A. Khan, P. Pillay, N. R. Batane, and D. J. Morrison, "Prototyping a composite SMC/steel axial-flux PM wind generator," in *Proc. Conf. Rec. IEEE Ind. Appl. Conf. 41st IAS Annu. Meeting*, Tampa, FL, USA, Oct. 2006, pp. 2374–2381, doi: 10.1109/IAS.2006.256873.

[7] D. Kowal, P. Sergeant, L. Dupre, and A. Van den Bossche, "Comparison of nonoriented and grain-oriented material in an axial flux permanent-magnet machine," *IEEE Trans. Magn.*, vol. 46, no. 2, pp. 279–285, Feb. 2010.

[8] H.-J. Pyo, J. W. Jeong, J. Yu, S. G. Lee, and W.-H. Kim, "Design of 3D-printed hybrid axial-flux motor using 3D-printed SMC core," *IEEE Trans. Appl. Supercond.*, vol. 30, no. 4, pp. 1–4, Jun. 2020, doi: 10.1109/TASC.2020.2973364.

[9] M. A. Grande, L. Ferraris, F. Franchini, and E. Poškovic, "New SMC materials for small electrical machine with very good mechanical properties," *IEEE Trans. Ind. Appl.*, vol. 54, no. 1, pp. 195–203, Jan. 2018.

[10] K. Izumiya, "Axial-flux machine using ferrite PM and round wire competitive to radial-flux machine using Nd-Fe-B PM for HEV traction," in *Proc. IEEE Int. Conf. Electr. Mach. (ICEM)*, Oct. 2022, pp. 192–198.

[11] Y. Guo, J. Zhu, D. Dorrell, H. Lu, and Y. Wang, "Development of a claw pole permanent magnet motor with a molded low-density soft magnetic composite stator core," in *Proc. IEEE Energy Convers. Congr. Expo.*, San Jose, CA, USA, Sep. 2009, pp. 294–301, doi: 10.1109/ECCE.2009.5316258.

[12] Q. Chen, D. Liang, S. Jia, Q. Ze, and Y. Liu, "Analysis of winding MMF and loss for axial flux PMSM with FSCW layout and YASA topology," *IEEE Trans. Ind. Appl.*, vol. 56, no. 3, pp. 2622–2635, May 2020, doi: 10.1109/TIA.2020.2981445.

[13] L. Xu, Y. Xu, and J. Gong, "Analysis and optimization of cogging torque in yokeless and segmented armature axial-flux permanent-magnet machine with soft magnetic composite core," *IEEE Trans. Magn.*, vol. 54, no. 11, pp. 1–5, Nov. 2018, doi: 10.1109/TMAG.2018.2850317.

[14] G. De Donato, F. G. Capponi, G. A. Rivellini, and F. Caricchi, "Integral-slot versus fractional-slot concentrated-winding axial-flux permanent-magnet machines: Comparative design, FEA, and experimental tests," *IEEE Trans. Ind. Appl.*, vol. 48, no. 5, pp. 1487–1495, Sep. 2012.

[15] L. Shao, R. Navaratne, M. Popescu, and G. Liu, "Design and construction of axial-flux permanent magnet motors for electric propulsion applications—A review," *IEEE Access*, vol. 9, pp. 158998–159017, 2021, doi: 10.1109/ACCESS.2021.3131000.

[16] L. L. Evangelista, D. S. Avila, M. A. Carvalho, H. D. Lopes, and P. A. P. Wendhausen, "Mechanical strength and energy losses optimization of Somaloy 3P 700-based components," *IEEE Trans. Magn.*, vol. 52, no. 5, pp. 1–4, May 2016.

[17] J. Washington, S. Jordan, and L. Sjöberg, "Methods for the construction of single-sided axial flux machines using soft magnetic composites," in *Proc. IEEE Energy Convers. Congr. Expo. (ECCE)*, Portland, OR, USA, Oct. 2018, pp. 3278–3285, doi: 10.1109/ECCE.2018.8557658.

[18] R. Tsunata, M. Takemoto, S. Ogasawara, T. Saito, and T. Ueno, "SMC development guidelines for axial flux PM machines employing coreless rotor structure for enhancing efficiency based on experimental results," *IEEE Trans. Ind. Appl.*, vol. 58, no. 3, pp. 3470–3485, May 2022, doi: 10.1109/TIA.2022.3154336.

[19] L. Ferraris, P. Ferraris, E. Poskovic, and A. Tenconi, "Theoretic and experimental approach to the adoption of bonded magnets in fractional machines for automotive applications," *IEEE Trans. Ind. Electron.*, vol. 59, no. 5, pp. 2309–2318, May 2012.

[20] R. Tsunata, M. Takemoto, S. Ogasawara, A. Watanabe, T. Ueno, and K. Yamada, "Investigation of enhancing efficiency and acceleration in a flat shape axial gap motor having high torque characteristic," in *Proc. IEEE Int. Conf. Mechatronics (ICM)*, Feb. 2017, pp. 278–283.

[21] H. Lu, J. Li, R. Qu, D. Ye, and L. Xiao, "Reduction of unbalanced axial magnetic force in postfault operation of a novel six-phase double-stator axial-flux PM machine using model predictive control," *IEEE Trans. Ind. Appl.*, vol. 53, no. 6, pp. 5461–5469, Nov. 2017.

[22] T. D. Nguyen, K.-J. Tseng, S. Zhang, and H. T. Nguyen, "A novel axial flux permanent-magnet machine for flywheel energy storage system: Design and analysis," *IEEE Trans. Ind. Electron.*, vol. 58, no. 9, pp. 3784–3794, Sep. 2011.

[23] W. Deng and S. Zuo, "Axial force and vibroacoustic analysis of external-rotor axial-flux motors," *IEEE Trans. Ind. Electron.*, vol. 65, no. 3, pp. 2018–2030, Mar. 2018.

REN TSUNATA (Member, IEEE) was born in Miyagi, Japan, in 1992. He received the B.S., M.S., and Ph.D. degrees in electrical engineering from Hokkaido University, Hokkaido, Japan, in 2015, 2017, and 2021, respectively.

From 2017 to 2018, he was with Toyota Motor Corporation, Aichi, Japan. In 2021, he joined Okayama University, Okayama, Japan, as a Research Fellow. Since 2022, he has been an Assistant Professor with the Graduate School of Natural Science and Technology, Okayama University. His research interests include permanent magnet synchronous machines, variable flux motors, and axial flux machines. He is a member of the Institute of Electrical Engineers of Japan (IEEJ) and the Japan Society of Applied Electromagnetics and Machines (JSAEM). He was a recipient of four IEEJ Excellent Presentation Awards, in 2017, 2020, and 2022, and the Incentive Award from JSAEM, in 2020.

MASATSUGU TAKEMOTO (Member, IEEE) was born in Tokyo, Japan, in 1972. He received the B.S. and M.S. degrees in electrical engineering from the Tokyo University of Science, Noda, Japan, in 1997 and 1999, respectively, and the Ph.D. degree in electrical engineering from the Tokyo Institute of Technology, Tokyo, in 2005.

In 1999, he joined the Department of Electrical Engineering, Tokyo Institute of Technology, as a Research Associate. In 2004, he joined the Department of Mechanical Systems Engineering, Musashi Institute of Technology, Tokyo, as a Research Associate, where he became a Lecturer, in 2005. In 2008, he joined the Graduate School of Information Science and Technology, Hokkaido University, Sapporo, as an Associate Professor. Since 2020, he has been with Okayama University, Okayama, Japan, where he is currently a Professor with the Graduate School of Natural Science and Technology. His research interests include permanent magnet synchronous motors, axial gap motors, rare-earth-free motors, bearingless motors, and magnetic bearings. He is a member of IEEJ. He was a recipient of the Nagamori Award from the Nagamori Foundation, in 2017, the IEEJ Transaction Paper Award, in 2005, the Prize Paper Awards from the Electric Machines Committee of the IEEE Industry Applications Society, in 2011 and 2019, and the Prize Paper Award from the Electrical Machines Technical Committee of the IEEE Industrial Electronics Society, in 2018. He has served as a Secretary, the Vice Chair, and the Chair of the IEEE IAS Japan Chapter, from 2008 to 2009, from 2010 to 2011, and from 2012 to 2013, respectively.

JUN IMAI (Member, IEEE) was born in Okayama, Japan, in 1964. He received the B.S., M.S., and Ph.D. degrees in electrical engineering from the Department of Electrical Engineering, Kyushu University, in 1987, 1989, and 1992, respectively. In 2000, he became a Lecturer with Okayama University, where he has been an Associate Professor, since 2008. His major research interest includes modeling and control of distributed parameter systems, especially in performance limitation issues of physical control systems.

TATSUYA SAITO was born in Kyoto, Japan, in 1987. He received the B.S., M.S., and Ph.D. degrees in material science from Tohoku University, Sendai, Japan, in 2009, 2011, and 2014, respectively. Since 2014, he has been with Sumitomo Electric Industries Ltd., Hyogo, Japan, where he is engaged in research on soft magnetic materials and powder metallurgy.

TOMOYUKI UENO was born in Wakayama, Japan, in 1976. He received the B.S. and M.S. degrees in mechanical engineering from Kobe University, Hyogo, Japan, in 1999 and 2001, respectively, and the Dr.Eng. degree in industrial innovation science from Okayama University, in 2015. Since 2001, he has been with Sumitomo Electric Industries Ltd., where he is engaged in research on soft magnetic materials, ceramic materials, and cutting and grinding technology. He is a member of the Japan Society and Power Metallurgy (JSPM) and the Japan Society for Abrasive Technology (JSAT). He was a recipient of the JSPM Award for Innovatory Research, in 2009, the JSAT Prize Paper Award, in 2012, the Prize Paper Award from the Machine Tool Engineer Foundation, in 2012, and the JSPM Award for Innovatory Development, in 2013.